

# Cation Transport in Polymer Electrolytes: A Microscopic Approach

A. Maitra and A. Heuer

Westfälische Wilhelms-Universität Münster, Institut für Physikalische Chemie, Corrensstr. 30, 48149 Münster, Germany and  
NRW Graduate School of Chemistry, Corrensstr. 36, 48149 Münster, Germany

(Dated: May 27, 2019)

A microscopic theory for cation diffusion in polymer electrolytes is presented. Based on a thorough analysis of molecular dynamics simulations on PEO with  $\text{LiBF}_4$  the mechanisms of cation dynamics are identified and related to the polymer dynamics. The polymer itself is well described by the Rouse theory. The concept of *renewal* processes, as used in previous phenomenological approaches, is validated and allows one to rephrase the numerical observations in terms of an analytical expression for the lithium ion diffusion coefficient  $D_{Li}$ . In particular, the chain length dependence of  $D_{Li}$  can be predicted and compared with experimental data. This dependence can be fully understood without referring to entanglement effects.

PACS numbers: 61.20.Qg, 61.25.Hq, 66.10.Ed

The cation transport in complex systems is of major relevance in the field of disordered ion conductors. Specifically, polymer electrolytes [1, 2, 3], using lithium salts, have been intensively studied experimentally and theoretically due to their technological relevance. Free lithium ions ( $\text{Li}^+$ ), uncomplexed by the anions, are the desirable charge carriers in electrolytic applications. A theoretical description of ionic dynamics in terms of microscopic properties is difficult because the dynamics of the cations and the polymer segments occur on the same time scale [4, 5]. In contrast, the dynamics of ions in inorganic systems can be characterized by ionic hops between permanent sites, supplied by the immobile network [6].

Computer simulations [5, 7, 8, 9, 10, 11, 12] have been a very fruitful approach to elucidate the mechanisms of cation dynamics [8]. Recently, Borodin and Smith [13] have estimated the  $\text{Li}^+$  diffusion constant  $D_{Li}$  on the basis of a Monte-Carlo simulation, using a lattice model. The model ingredients were extracted from microscopic simulations of a polymer electrolyte. They were able to qualitatively assess the relevance of the variety of cation transport mechanisms that contribute to the macroscopic cation diffusivity. A different approach has been taken in the phenomenological dynamic bond-percolation model (DBP) [14]. The key-concept for long-range ion transport to be feasible is the presence of *renewal* events which lift the blockage in the ion-pathways. Since the dynamics after a renewal event is statistically uncorrelated to its past, the resulting diffusion constant can be written as  $D_{Li} = a_{Li}^2/6\tau_{renewal}$  where  $a_{Li}^2$  denotes the typical mean square displacement (MSD) between two renewal events. In this model the renewal process is attributed to a local structural relaxation process with a rate  $1/\tau_{renewal}$ , governed by the polymer dynamics. This gives  $D_{Li} \propto 1/\tau_{renewal}$ .

In this work we combine these different approaches in a two-step process. First, we identify the microscopic mechanisms of the cation transport from the analysis of very long molecular dynamics (MD)[15] simulations of a simple model system composed of a salt in a linear

polymer melt. One crucial aspect is to identify the renewal process and, for the first time, validate its statistical implications. Second, observations from simulations are translated into a microscopic model that expresses  $D_{Li}$  explicitly in terms of the microscopic parameters, extracted in the first step. Here the presence of the renewal process is essential. Since the  $N$ -scaling ( $N$ : number of monomers per chain) of these parameters is known we can, among others, obtain an improved understanding of the  $N$ -dependence of  $D_{Li}$  and the relevance of the different modes of transport to  $D_{Li}$ .

Atomistic NVT MD simulations are performed for the system poly(ethylene) oxide (PEO) and  $\text{LiBF}_4$  with a concentration of  $\text{EO}:\text{Li}=20:1$  (EO: ether oxygen). The two body effective polarizable potential employed is described in Ref. [5]. We have simulated this system for different chain lengths ( $N = 24$  and  $N = 48$ ) and at different temperatures ( $400 \text{ K} \leq T \leq 450 \text{ K}$ ). The respective densities have been adjusted to the experimental values. This letter discusses the results for the  $N=48$  system at  $T = 450 \text{ K}$  unless specified otherwise.

As has been observed before [5, 7, 9, 10] the  $\text{Li}^+$  ion is, most of the time, coordinated to a single polymer chain through EO atoms, interrupted by infrequent transitions between different chains. This suggests to map the ion dynamics to the properties of the polymer dynamics. More specifically, the ionic dynamics can be divided into three important mechanisms: (M1) motion along a chain ("intra-chain"), (M2) motion together with chain segments, using the chain as a vehicle ("segmental"), and (M3) jumps between different chains ("inter-chain"); see also [13]. This is sketched in Fig.1. The dynamics of a polymer segment can be separated into statistically uncorrelated center-of-mass (c.o.m) dynamics of the respective polymer chain (Rouse mode,  $p = 0$ ) and internal dynamics ( $p > 0$ ). For the  $\text{Li}^+$  ions this implies  $D_{Li} = D_{c.o.m} + D_M$  where  $D_M$  accounts for the contributions due to (M1)-(M3). We will describe  $D_M$  as a function of the time scales  $\tau_1$ ,  $\tau_2$  and  $\tau_3$  characterizing each of (M1)-(M3). The time scales are extracted from appropriate analyses of the MD trajectories.

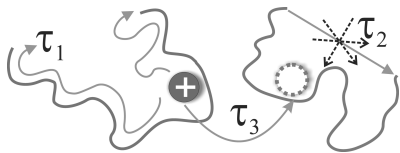


Figure 1: Time scales:  $\tau_1$  is the time scale for intra-chain ionic motion (M1),  $\tau_2$  is the relaxation time of the polymer chain (related to  $\tau_R$ : see text for details)(M2), and  $\tau_3$  is the waiting time of an ion between two inter-chain jumps (M3).

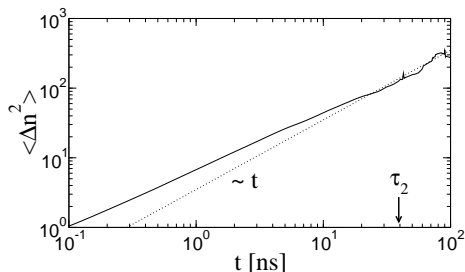


Figure 2: Average square variation of the average oxygen index of one chain to which a  $\text{Li}^+$  is associated during time interval  $t$ .

A  $\text{Li}^+$  ion which is bound to a polymer chain is coordinated to a few ( $\approx 5$ ) and mostly contiguous oxygen atoms. After serially indexing the oxygen atoms of a chain in succession we mark the position of the  $\text{Li}^+$  at the chain by the average index,  $n(t)$ , of the enumerated oxygen atoms that belong to its coordination sphere. To elucidate (M1), we determine the average-square variation  $\langle \Delta n(t)^2 \rangle$  of the average oxygen index under the constraint that the  $\text{Li}^+$  ion is attached to the same chain during the time interval of length  $t$ . The result is shown in Fig.2. To a good approximation one observes diffusive dynamics  $\langle \Delta n(t)^2 \rangle = 2D_1 t$  where  $D_1$  is the intra-chain ionic diffusivity. To account for the slight deviations from linear behavior we choose  $D_1 = \langle \Delta n(\tau_2)^2 \rangle / 2\tau_2$  ( $\tau_2$  defined in the next paragraph). For later purposes we define

$$\tau_1 = (N - 1)^2 / \pi^2 D_1 \quad (1)$$

where  $\tau_1$  is a measure of the time it takes for the lithium ion to diffuse from one end to the other end of the polymer chain. Here we obtain  $\tau_1 \approx 150$  ns (with  $D_1$  from Fig.2).

To characterize (M2) we first analyze the polymer dynamics. In Fig.3(a) we display the MSD  $g_O(t)$  for an average oxygen atom (i.e. all oxygen atoms were considered for analysis irrespective of the presence or absence of  $\text{Li}^+$  near an oxygen atom), characterizing the dynamics of the polymer segments. According to our general procedure all MSD-functions are computed relative to the polymer c.o.m. It exhibits the expected Rouse-behavior for short times  $g_O(t) \propto t^\alpha$  with  $\alpha \approx 0.6$ , saturating at  $g_O(t) \approx R_e^2/3$  where  $R_e^2$  is the mean square end-to-end distance of the polymer [16, 17]. We have included the theoretical Rouse prediction, obtained via numerical

summation

$$g(t/\tau_R) = \frac{2R_e^2}{\pi^2} \sum_{p=1}^{N'} \frac{1 - \exp(-\frac{p^2 t}{\tau_R})}{p^2} \quad (2)$$

( $\tau_R$ : Rouse time). The sum is over the  $N' = (N - 1)/l_p$  eigenmodes (persistent length [18]  $l_p \approx 1.7$ ). It yields a reasonable description of the observed MSD, using  $\tau_R = 18$  ns; see also [19]. Qualitatively, it is expected that the oxygen atoms which are temporarily bound to a  $\text{Li}^+$  ion ought to be somewhat slower due to the decrease in the local degrees of freedom. This was checked by calculating  $g_O^{\text{bound}}(t)$  for those oxygen atoms which, during the whole time interval of length  $t$ , are bound to one  $\text{Li}^+$  ion. Indeed,  $g_O^{\text{bound}}(t)$  is also consistent with the Rouse prediction, using a longer Rouse time  $\tau_2 = 37.4$  ns. Naturally,  $\tau_2/\tau_R > 1$  reflects the immobilization of the polymer segments due to the ions. Note that for longer  $t$  less oxygen atoms contribute to this curve so that the statistics gets worse.

Switching to the  $\text{Li}^+$  dynamics, we first calculate the MSD  $g_{Li}^{M2}(t)$  of  $\text{Li}^+$  ions for which  $|n(t) - n(0)| \leq 1$ ; see Fig.3(a). For  $t > 2$  ns this curve is close to  $g_O^{\text{bound}}(t)$ . Thus, we can conclude that the  $\text{Li}^+$  motion strictly follows the oxygen dynamics in the absence of (M1). In other words, the cations and the polymer segments exhibit coupled dynamics. Additionally, we find (surprisingly) that for shorter times the  $\text{Li}^+$  ions are slower than the corresponding oxygen atoms.

In the absence of ion jump events between chains (M3) one would have  $D_M = 0$ . We have identified these jumps from a microscopic analysis of the trajectories. On average after  $\tau_3 = 110$  ns a  $\text{Li}^+$  ion jumps between two chains. To characterize the effect of these jumps we have first determined  $g_{Li}^{M123}(t)$  which is the MSD of a  $\text{Li}^+$  ion between times  $[t_0 - t, t_0 + t]$  if at time  $t_0$  a jump happens and during the intervals  $[t_0 - t, t_0]$  and  $[t_0, t_0 + t]$  the ion stays with the same chain, respectively. The MSD is averaged over all jumps (Fig.3(b)). Furthermore we have determined the MSD  $g_{Li}^{M12}(t)$  during the intervals  $[t_0 - t, t_0]$  or  $[t_0, t_0 + t]$ , i.e. just before or after an inter-chain jump, respectively. If the inter-chain jump serves as a renewal process, the statistical independence of the dynamics before and after the jump implies  $g_{Li}^{M123}(t) = 2g_{Li}^{M12}(t)$ . In case of correlations a smaller factor is expected in the present case. As exhibited in Fig.3b this relation is indeed found with minor deviations (prefactor 2.2 instead of 2.0), thus validating the concept of a renewal process on the level of inter-chain transitions.

In the following, we derive an explicit expression  $D_M = D_M(\tau_1, \tau_2, \tau_3)$ . Based on the observed correlations between a  $\text{Li}^+$  ion and the polymer dynamics,  $g_{Li}^{M12}(t)$  can be described by taking into account the Rouse dynamics (M2) plus the additional intra-chain diffusion (M1). Formally, one can write

$$g_{Li}^{M12}(t) = \langle (\vec{r}_j(t) - \vec{r}_i(0))^2 \rangle_{M12} \quad (3)$$

The average is over the probability density that the initial oxygen index to which an ion is linked is  $i$  and at a

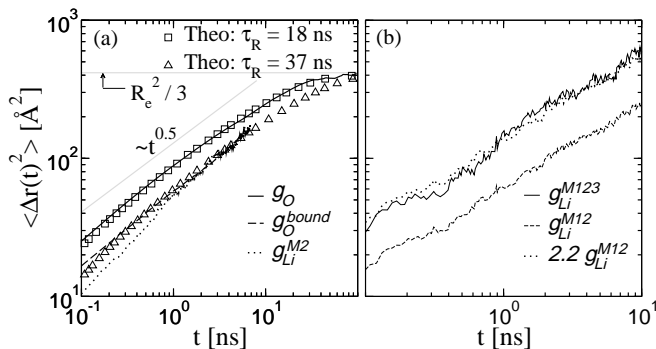


Figure 3: (a) MSD of (i) all oxygen atoms (solid), (ii) oxygen atoms which are bound to one  $Li^+$  during time duration  $t$  (dash), (iii)  $Li^+$  which changed the average index of its oxygen neighbors by at most 1 (dot). Also shown are the Rouse predictions with  $\tau_R=18$  ns ( $\square$ ) and  $\tau_R=37.4$  ns ( $\triangle$ ). (b) MSD of  $Li^+$  under different constraints (see text).

time  $t$  later is  $j$  and the distribution of monomer displacements as predicted in the Rouse theory. From Ref.[17] one obtains, using  $\langle \cos^2(p\pi(j-0.5)/N) \rangle_{M1} = 1/2$  and  $\langle \cos(p\pi(i+j-1)/N) \rangle_{M1} = 0$ ,

$$g_{Li}^{M12}(t) = \frac{2R_e^2}{\pi^2} \sum_{p=1}^{N'} \frac{1 - \langle \cos \frac{p\pi(i-j)}{N} \rangle_{M1} \exp(-\frac{p^2 t}{\tau_2})}{p^2}. \quad (4)$$

Assuming Gaussian dynamics for (M1), i.e.  $\langle \Delta n^2 \rangle \propto t$  (corrections as observed in Fig.2 can be easily implemented but are not of relevance here), one finds  $\langle \cos(p\pi(i-j)/N) \rangle_{M1} = \exp(-p^2 t/\tau_1)$ . Eq. 4 simplifies to (using Eq.2)

$$g_{Li}^{M12}(t) = g(t/\tau_{12}) \quad (5)$$

with  $1/\tau_{12} = 1/\tau_1 + 1/\tau_2$ . Thus, the dynamical effects of (M1) and (M2) appear through the resulting relaxation rate  $1/\tau_{12}$ . Finally, using the renewal property one can write  $D_M = a_M^2/6\tau_3$  more explicitly as

$$D_M = \langle g_{Li}^{M12}(\tau) \rangle_{M3}/6\tau_3 \quad (6)$$

where  $a_M^2$  corresponds to the average MSD between successive inter-chain hopping events due to (M1) and (M2). The average is taken over the distribution of time intervals between these events. For the numerical analysis (see below) we take a simple exponential distribution.

Approximate analytical expressions can be obtained by converting the sum in Eq.4 into an integral from 0 to  $\infty$  [17]. Then one obtains  $g_{Li}^{M12} = 2R_e^2\pi^{-3/2} \sqrt{t/\tau_{12}}$  for  $t \ll \tau_{12}$  and  $g_{Li}^{M12} = R_e^2/3$  for  $t \gg \tau_{12}$ , respectively. Inserting these results into Eq.6 gives

$$D_M = \frac{R_e^2}{6\pi} \sqrt{\frac{1}{\tau_3\tau_{12}}} \quad \text{if } \tau_3 \ll \tau_{12} \quad (7a)$$

$$= \frac{R_e^2}{18\tau_3} \quad \text{if } \tau_3 \gg \tau_{12} \quad (7b)$$

The scaling of  $D_M$  with  $\tau_3$  in Eq.(7a) is consistent with the numerical results, obtained in Ref.[13]. Eq.(7a) holds

$N$	$\tau_1$ [ns]	$\tau_2$ [ns]	$\tau_3$ [ns]
48	150	37	110
24	35 (40)	9 (10)	90 (110)

Table I: The relevant time scales  $\tau_i$  for  $N = 48$  and  $N = 24$  as well as a check of the scaling relations.

for long chains and takes into consideration the implicit correlations of (M1) and (M2). By neglecting these correlations, as done in Ref.[13], the term  $\sqrt{1/\tau_{12}} = \sqrt{1/\tau_1 + 1/\tau_2}$  would instead become  $\sqrt{1/\tau_1} + \sqrt{1/\tau_2}$ . This would largely overestimate  $D_M$  (for instance, in PEO/LiBF<sub>4</sub> by 35 %) and the contribution of (M1) for the case  $\tau_3 \ll \tau_{12}$ .

In contrast to the DBP-model we obtain  $D_M \propto 1/\tau_{renewal}$  only for short chains. The main conclusion, however, that the  $Li^+$  diffusion has the same temperature dependence as the inverse Rouse time and thus as the polymer dynamics, remains valid because all the three time scales  $\tau_i$  have a similar temperature dependence (data not shown).

In Tab.I we have compiled  $\tau_1, \tau_2, \tau_3$ , obtained from our simulations for  $N = 24$  and  $N = 48$ . Of major importance are their scaling properties with  $N$ . One expects  $\tau_1, \tau_2 \propto N^2$  and  $\tau_3 \propto N^0$ . Considering the appropriate number of eigenmodes, the predictions for  $N = 24$ , based on  $N = 48$ , are given in parenthesis. The agreement is convincing. By setting  $\tau_1 = \infty$  one can estimate the contribution of (M1) to  $D_M$  in the limit of long chains ( $\tau_3 \ll \tau_{12}$ ). It is as small as 12% for the present system.

Naively one might expect that  $a_M^2 \propto N^0$  and thus  $D_M \propto N^0$  for all  $N$ , see e.g. [20], because (M1)-(M3) are related to local motions. Using the scaling results for the  $\tau_i$  one obtains, however,  $D_M \propto N^0$  only for long chains ( $\tau_3 \ll \tau_{12}$ ) whereas  $D_M \propto N$  for short chains. The reason is that for short chains  $a_M^2$  is limited by the end-to-end distance of the polymer which brings an  $N$ -dependence.

In the present case, the crossover in  $D_M$ , i.e.  $\tau_3 \approx \tau_{12}$ , occurs for  $N \approx 100$  (see inset of Fig.4). It has been speculated [20] that the emergence of the entanglement regime ( $N \approx 75$  [20, 21]) leads to the crossover with an accompanying change of cation conduction process from polymer c.o.m dominated motion to percolation type transport (i.e. (M3)). However, we find, it is a coincidence that the entanglement length is similar to the crossover length. Thus, the crossover to  $D_M \propto N^0$  is physically unrelated to entanglement effects.

We can predict the  $N$ -dependence of  $D_{Li}(N)$  for a large range of  $N$  values by combining the empirical  $N$ -scaling [22, 23] (see inset Fig.4) of  $D_{c.o.m}(N)$  with  $D_M(N)$ . The Rouse scaling ( $D_{c.o.m} \propto N^{-1}$ ) is known to be violated and substantially higher exponents ( $\geq 1.5$ ) have been reported [22, 23, 24].

To determine  $D_M(N)$  we have used Eq.5 and 6 by explicitly calculating the sum in Eq.4. Fig.4 displays the predicted  $D_{Li}(N)$  along with the experimental data from Ref.[20]. In agreement, both indicate a transition to a  $N$ -independent regime beyond  $N \approx 100$ . Further included

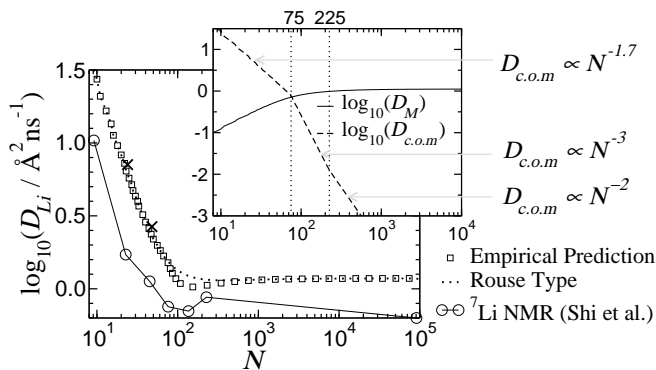


Figure 4: Self diffusivity of  $\text{Li}^+$ ,  $D_{Li} = D_M + D_{c.o.m}$  with  $D_M$  from Eq.6 ( $\square$ ). The dotted line shows the prediction for a pure Rouse-type motion. Experimental  $D_{Li}$  for PEO: $\text{LiCF}_3\text{SO}_3$  with EO: $\text{Li}$ =20:1 at  $T=342$  K is included ( $\circ$ ). The inset shows  $D_M$  and  $D_{c.o.m}$  individually.  $D_{Li}$  values obtained from simulations are marked by crosses.

in Fig.4 is an estimation of  $D_{Li}$  under the assumption that no entanglement effects are present for  $D_{c.o.m}$  by simply extending the scaling in the Rouse-regime to all  $N$ . As expected, the large- $N$  behavior does not depend on the specific form of  $D_{c.o.m}$ . However, one might speculate that the appearance of the minimum in  $D_M(N)$  is indicative of entanglement effects.

Interestingly, within the present approach the value of  $\tau_3$  can be estimated from experimental data. For very large  $N = N_L$  one has (see Eq.(7a))  $\tau_3 = (N_s b^2 / (6\pi D_{Li}|_{N=N_L}))^2 / (\tau_R|_{N=N_s})$  where  $b^2$  is the effective bond length of the polymer [18] and  $\tau_R|_{N=N_s}$  can be estimated from  $D_{c.o.m} \approx D_{Li}|_{N=N_s}$  (at some small

$N = N_s$ ) using the Rouse prediction. For the experimental data in Fig.4 this yields  $\tau_3 \approx 200$  ns.

It is likely that the identified motional mechanisms are generally applicable to understand the ionic dynamics in different polymer electrolytes. Furthermore we checked that the presence of a small fraction of ions which are, temporarily, not bound to a polymer does not change the value of  $D_M$  by more than 10%. Of course, corrections will become relevant for larger ion concentration due to their mutual interaction. An extension is planned to topologically more complex systems like polyphosphazene to understand the large conductivities in these systems.

In summary, we have elucidated ion dynamics in polymer electrolytes by extracting microscopic properties from simulation and expressing them in analytical terms. This extends previous phenomenological approaches like the dynamic bond-percolation model, by assigning its key concept, i.e. the presence of *renewal* processes, a specific microscopic interpretation. For long chains the scaling relation  $D_{Li} \propto 1/\sqrt{\tau_{12} \cdot \tau_3}$  is obtained which goes beyond the expressions from the DBP model. In any event, for the transport of lithium ions fast transitions of ions between different chains are vital. Since the expression  $D_{Li}(\tau_1, \tau_2, \tau_3)$  is now available one can estimate the possible range of ionic mobilities for polymer electrolytes for all  $N$ .

We would like to thank M. Vogel for important discussions and a critical reading of the manuscript and Y. Aihara, J. Baschnagel, O. Borodin, K. Hayamizu, and M. Ratner for helpful correspondence.

- 
- [1] F. M. Gray, *Solid Polymer Electrolytes* (Wiley-VCH, New York, 1991).
- [2] P. G. Bruce and C. A. Vincent, *J. Chem. Soc. Faraday Trans.* **89**, 3187 (1993).
- [3] M. A. Ratner and D. F. Shriver, *Chem. Rev.* **88**, 109 (1988).
- [4] M. Ratner, P. Johansson, and D. Shriver, *MRS Bulletin* **25**, 31 (2000).
- [5] O. Borodin, G. D. Smith, and R. Douglas, *J. Phys. Chem. B* **107**, 6824 (2003).
- [6] H. Lammert, M. Kunow, and A. Heuer, *Phys. Rev. Lett.* **90**, 215901 (2003).
- [7] O. Borodin and G. D. Smith, *Macromolecules* **31**, 8396 (1998).
- [8] O. Borodin and G. D. Smith, *Macromolecules* **33**, 2273 (2000).
- [9] S. Neyertz and D. Brown, *J. Chem. Phys.* **104**, 3797 (1996).
- [10] F. Müller-Plathe and W. van Gunsteren, *J. Chem. Phys.* **103**, 4745 (1995).
- [11] F. Müller-Plathe, *Acta Polymer.* **45**, 259 (1994).
- [12] L. J. A. Siqueira and M. Ribeiro, *J. Chem. Phys.* **125**, 214903 (2006).
- [13] O. Borodin and G. D. Smith, *Macromolecules* **39**, 1620 (2006).
- [14] A. Nitzan and M. A. Ratner, *J. Phys. Chem.* **98**, 1765 (1994).
- [15] M. P. Allen and D. J. Tildesley, *Computer Simulation of Liquids* (Clarendon, Oxford, 2004).
- [16] P. E. Rouse, *J. Chem. Phys.* **21**, 1272 (1953).
- [17] M. Doi and S. Edwards, *The Theory of Polymer Dynamics* (Oxford Science Publications, 2003).
- [18] After Flory:  $b^2 = b_o^2 l_p^2 = R_e^2 / (N - 1)$  where  $b^2$  is the statistical segment length of the polymer and  $b_o^2$  is the mean square distance between contiguous oxygen atoms.
- [19] T. Kreer, J. Baschnagel, M. Müller, and K. Binder, *Macromolecules* **34**, 1105 (2001).
- [20] J. Shi and C. A. Vincent, *Solid State Ionics* **60**, 11 (1993).
- [21] M. Appel and G. Fleischer, *Macromolecules* **26**, 5520 (1993).
- [22] E. von Meerwall, S. Beckman, J. Jang, and L. Mattice, *J. Chem. Phys.* **108**, 4299 (1998).
- [23] K. Hayamizu, E. Akiba, T. Bando, and Y. Aihara, *J. Chem. Phys.* **117**, 5929 (2002).
- [24] W. Paul and G. D. Smith, *Rep. Prog. Phys.* **67**, 1117 (2004).